AD_____

Award Number: DAMD17-02-1-0072

TITLE: Targeting Nuclear Factor kappa B for the Treatment of Prostate Cancer

PRINCIPAL INVESTIGATOR: Christopher Sweeney

CONTRACTING ORGANIZATION: Indiana University
Indianapolis, IN 46202-5167

REPORT DATE: February 2005

TYPE OF REPORT: Final

PREPARED FOR: U.S. Army Medical Research and Materiel Command
Fort Detrick, Maryland 21702-5012

# REPORT DOCUMENTATION PAGE

Form Approved
OMB No. 0704-0188



| 1. REPORT DATE (DD-MM-YYYY) | 2. REPORT TYPE | 3. DATES COVERED (From - To) |
|---|---|---|
| 01/02/2005 | Final | 1 Feb 02 - 31 Jan 05 |

**4. TITLE AND SUBTITLE**
Targeting Nuclear Factor kappa B for the Treatment of Prostate Cancer

**5a. CONTRACT NUMBER**

**5b. GRANT NUMBER**
DAMD17-02-1-0072

**5c. PROGRAM ELEMENT NUMBER**

**6. AUTHOR(S)**
Christopher Sweeney

E-Mail: chsweene@iupui.edu

**5d. PROJECT NUMBER**

**5e. TASK NUMBER**

**5f. WORK UNIT NUMBER**

**7. PERFORMING ORGANIZATION NAME(S) AND ADDRESS(ES)**
Indiana University
Indianapolis, IN 46202-5167

**8. PERFORMING ORGANIZATION REPORT NUMBER**

**9. SPONSORING / MONITORING AGENCY NAME(S) AND ADDRESS(ES)**
U.S. Army Medical Research and Materiel Command
Fort Detrick, Maryland 21702-5012

**10. SPONSOR/MONITOR'S ACRONYM(S)**

**11. SPONSOR/MONITOR'S REPORT NUMBER(S)**

**12. DISTRIBUTION / AVAILABILITY STATEMENT**
Approved for Public Release; Distribution Unlimited.

**13. SUPPLEMENTARY NOTES**

**14. ABSTRACT**

This report details the work conducted as part of the New Investigator Award. In essence, we have shown the relevance of the the transcription factor, Nuclear Factor kappa B (NFκB) to prostate cancer and that inhibition with parthenolide results in anti-cancer activity. To date we have shown that NFκB is constitutively active in prostate cancer cell lines and endothelial cells and that NFκB DNA binding is inhibited by parthenolide. Moreover, we have found that NFκB is over-expressed in human prostatectomy specimens at both the prostatic intraepithelial neoplasia and invasive adenocarcinoma stages. With the use of cDNA array technology we have shown that multiple genes associated with the hallmarks of cancer and that are under NFκB control are decreased when cancer and endothelial cells are treated with parthenolide. Western blot analysis confirmed these findings at the protein level. We have subsequently shown that parthenolide is able to decrease cancer cell proliferation and enhance the cytotoxic effect of taxanes *in vitro*. Finally, we have shown that parthenolide is bioactive *in vivo* as it is able to inhibit angiogenesis as a single agent, enhance the cytotoxic effects of docetaxel and restore sensitivity of the hormone independent cell line, CWR22Rv1, to the anti-androgen, bicalutamide. More recently, we demonstrated the ability of parthenolide to activate JNK *in vitro* and *in vivo*. However, our *in vivo* work in collaboration with the NCI through the RAID program revealed the poor oral biovailability of parthenolide. With these findings in hand, we have directed our efforts to developing a water soluble analogue that will be more suitable for clinical development as well as turning our attention to defining the drug's mechanism of action.

**15. SUBJECT TERMS**
Nuclear Factor kappa B, prostate cancer, parthenolide

| 16. SECURITY CLASSIFICATION OF: | | | 17. LIMITATION OF ABSTRACT | 18. NUMBER OF PAGES | 19a. NAME OF RESPONSIBLE PERSON |
|---|---|---|---|---|---|
| a. REPORT | b. ABSTRACT | c. THIS PAGE | | | 19b. TELEPHONE NUMBER (include area code) |
| U | U | U | UU | 23 | |

Standard Form 298 (Rev. 8-98)
Prescribed by ANSI Std. Z39.18

## Table of Contents

**INTRODUCTION:**

This report details our accomplishments over the three year period covered by the award. We have shown that NFκB is constitutively active in prostate cancer cell lines and endothelial cells and that NFκB DNA binding is inhibited by parthenolide. Moreover, we have found that NFκB is over-expressed in human prostatectomy specimens at both the prostatic intraepithelial neoplasia and invasive adenocarcinoma stages. With the use of cDNA array technology we have shown that multiple genes associated with the hallmarks of cancer and that are under NFκB control are decreased when cancer and endothelial cells are treated with parthenolide. We have subsequently confirmed these findings at the protein level with Western blot analysis. We have subsequently shown that parthenolide is able to decrease cancer cell proliferation and enhance the cytotoxic effect of taxanes *in vitro*. Finally, we have shown that parthenolide is bioactive *in vivo* as it is able to inhibit angiogenesis as a single agent, enhance the cytotoxic effects of docetaxel and restore sensitivity of the hormone independent cell line, CWR22Rv1, to the anti-androgen, bicalutamide. More recently, we demonstrated the ability of parthenolide to also activate JNK *in vitro* and *in vivo*. However, our *in vivo* work in collaboration with the NCI through the Rapid Access to Intervention Development (RAID) program revealed the poor oral biovailability of parthenolide. With these findings in hand, we have directed our efforts to developing a water soluble analogue that will be more suitable for clinical development as well as turning our attention to defining the drug's mechanism of action.

**BODY:**

**Task 1. To identify the relative amount of the NFκB p65:p50 heterodimer and the genes increased in response to greater NFκB activity in hormone refractory cells:**

*a) Culture hormone dependent(LNCaP) and hormone independent cells (C4-2)and perform a gel-shift analysis.*

*b) Perform the gel shift assay with cells treated with parthenolide.*

A notable function of parthenolide described by several investigators is its ability to inhibit NFκB[1-4]. NFκB is a collection of dimers composed of members of the Rel family of transcription factors. The most active NFκB dimer is the p65:p50 heterodimer. NFκB dimers are bound to inhibitory IκB proteins in the cytoplasm and are released from IκB after phosphorylation of IκB by IκKinase (IKK) by proteosome mediated degradation of IκB. The release of NFκB and subsequent binding to DNA occurs in response to a variety of stimuli including cytokines such as Tumor Necrosis Factor (TNF) and interleukin-1 (IL-1) which are found in the microenvironment of many cancers[5]. We have found *in vitro* that NFκB DNA binding is present in all prostate cancer cell lines evaluated (Figure 1). The proportion of the p65:p50 heterodimer to p50:p50 homodimer is lowest in the LNCaP cell lines that have undergone the least number of passages in culture compared with (i) the LNCaP cell lines that have undergone a higher number of passages and (ii) the hormone independent cell lines – C42 and PC-3 (Figure 1A). Also of note is that parthenolide is able to inhibit the NFκB DNA binding in a dose dependent manner starting at 0.5 μM. EMSA also showed that NFκB DNA binding is present in the androgen independent prostate cancer cell line, CWR22Rv1, and supershift confirmed the presence of the active subunit, p65. NFκB DNA binding was again inhibited by parthenolide (Figure 1B).

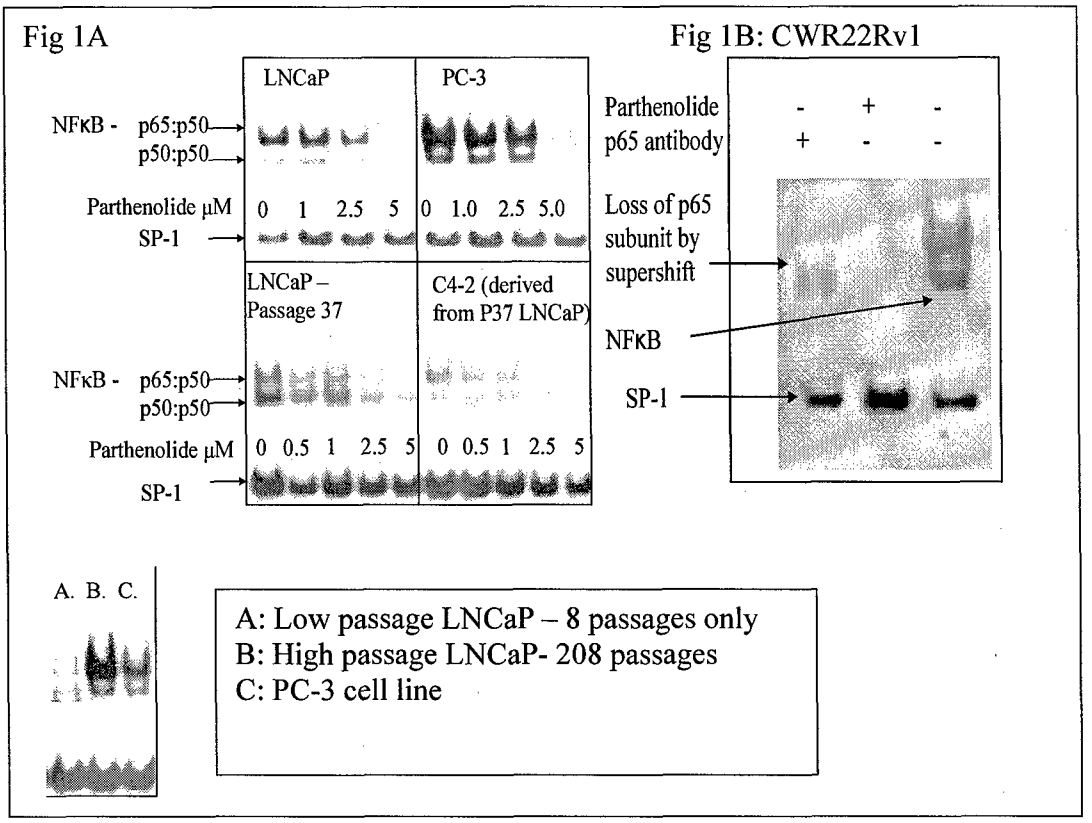


*c. Perform a ribonuclease protection assay to analyze for altered levels of gene expression.*

At the time writing this grant application we proposed to perform a global analysis of parthenolide's ability to suppress genes under NFκB control using the ribonuclease protection assay (RPA). We opted to perform the evaluation using a NFκB Superarray instead of the RPA as it assesses more genes under NFκB control and permits quantification of changes by image analysis. The rationale for this evaluation is the following: Genes activated by NFκB play a central role in many of the hallmarks of cancer including: *invasion* (IL-6, matrix metallaproteinase 9; *angiogenesis*: (IL-8, vascular endothelial growth factor [VEGF]); *organ specific homing of metastatic* cells (CXCR4); and *evasion of apoptosis*: (cIAP-1, c-IAP-2, TRAF-1, TRAF-2, Bfl-1/A1, Bcl-$X_L$ and manganese superoxide dismutase[6-11]. The relative expression level of 96 transcripts under NFκB control was determined before and after parthenolide treatment using chemiluminesence and the GEArray Analyzer. All results were normalized by adjusting for the signal derived from GAPDH and β-actin spots. The change in a given gene transcript from one experiment was estimated by comparing the signal intensities of paired specimens. Genes that had at least a two-fold decrease after 6 hours of treatment in both experiments and the average of the two was greater than four-fold were arbitrarily considered to show a magnitude and consistency in effect between experiments to support the hypothesis that genes under NFκB control are present in prostate cancer cells and provide relevance to the electromobility gel shift findings above. The 23 genes that met these criteria and are under the transcriptional control of NFκB [12] are detailed in Table

Figure 2
cDNA Array of CWR22Rv1 cells with and without 10 μM of parthenolide for 6 hours.

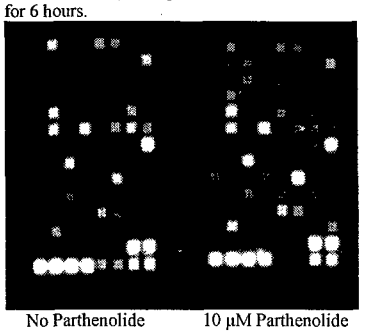

1. It is of note is that many of the genes associated with the hallmarks of cancer[13] were decreased. Specifically, genes associated with evasion of apoptosis, TNF receptor associated factor-1 (TRAF-1) and TRAF-5 were decreased. Also genes associated with maintaining cell-cell adhesion and thus preventing metastasis (ICAM-2, ICAM-5 and VCAM) and genes associated with "unlimited" growth (c-myc) were also decreased.

| **Table 1**<br>**Gene** | **Experiment 1*** | **Experiment 2*** | **Average of 1&2*** |
|---|---|---|---|
| Intercellular adhesion molecule 2 | 39 | 32 | 35.5 |
| Intercellular adhesion molecule 5, telencephalin | 47 | 80 | 63.5 |
| Interferon, alpha 1 | 53 | 32 | 42.5 |
| Interferon, beta 1, fibroblast | 33 | 12 | 22.5 |
| Interleukin 12B, p40 | 63 | 47 | 55 |
| Interleukin 1, alpha | 75 | 13 | 44 |
| Interleukin 1, beta | 52 | 44 | 48 |
| Interleukin-1 receptor type II | 16 | 44 | 30 |
| Interleukin-1 receptor-associated kinase (IRAK) mRNA | 60 | 17 | 38.5 |
| Lymphotoxin-alpha (TNF superfamily, member 1) | 46 | 60 | 53 |
| Protein kinase, mitogen-activated 3 (MAP kinase 3; p44) | 43 | 40 | 41.5 |
| Neural cell adhesion molecule 1 | 35 | 57 | 46 |
| Orosomucoid 1 (ORM1, alpha-1 acid glycoprotein ) | 53 | 51 | 52 |
| Transforming growth factor beta-activated kinase-binding protein 1 (TAB1), | 17 | 50 | 33.5 |
| Toll-like receptor 10 (TLR10), | 20 | 80 | 50 |
| Tumor necrosis factor (TNF superfamily, member 2) | 46 | 28 | 37 |
| TNF receptor-associated factor 1 | 40 | 29 | 34.5 |
| TNF receptor-associated factor 5 | 20 | 13 | 16.5 |

*d. Correlate the level of gene expression with changes in the corresponding protein.*
We focused our analysis on the anti-apoptotic proteins TRAF-1 and TRAF-2.

Figure 3

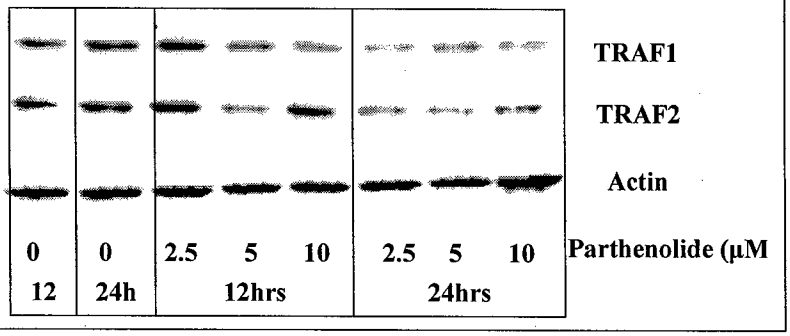


Given recent data suggesting the ability of parthenolide to activate c-Jun-N-terminal kinase (JNK), we also performed western blot analysis of this pathway as well. In essence, we found that not only

Figure 4

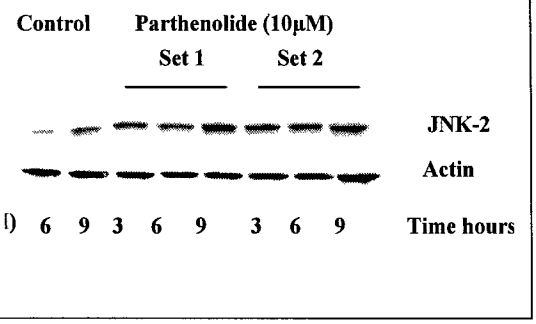


did parthenolide decrease proteins under NFkB control, it also activated the parallel pathway of JNK. The significance of this finding is unclear at this time and the subject of further evaluation beyond the scope of the current award. However, the following details how the tow paths are related and how decreasing NFkB, JNK may become activated. Specifically, the role JNK in apoptosis remains highly controversial, as it has been reported to have proapoptotic or antiapoptotic functions or no role depending on the cell type and stimulus. However, recent evidence supports the hypothesis that JNK plays a pro-apoptotic role especially when NFκB signaling is inhibited. Under such conditions sustained activation of JNK appears to be critical factor that determines the pro-apoptotic role of JNK. Activation of JNK and inhibition of NFκB have been found to interact in at least two points. Namely, both TRAF 1 and TRAF 2 have been implicated in decreasing JNK activation and in so doing preventing TNF induced apoptosis. The second interaction is the observation that NFκB mediated inhibition of GADD153 is also associated with JNK activation.

**This task is complete and a manuscript detailing these findings is in preparation and to be submitted to Cancer Research. Some of the data is also detailed in the attached Clinical Cancer Research paper.**

**Task 2. To identify the growth factors that increase NFκB activity in human umbilical venous endothelial cells and the genes that are increased in response to NFκB activity**

*a). Culture HUVECs and perform a gelshift analysis with solvent control, VEGF and bFGF*

*b). Perform the gel shift assay with cells treated with low dose parthenolide*

As can be seen in figure 5, NFκB DNA binding is present in HUVECS and can be increased by VEGF and bFGF and suppressed by parthenolide.

Figure 5:

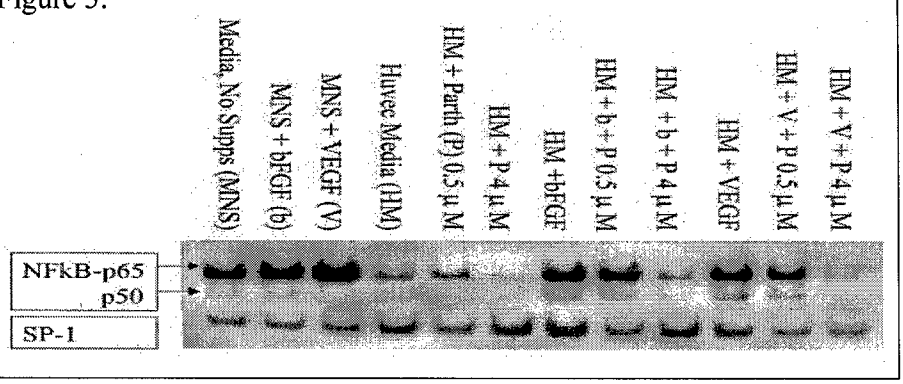

*c. Perform a ribonuclease protection assay to analyze for altered levels of gene expression.*

At the time of writing this grant application we proposed to perform a global analysis of parthenolide's ability to suppress genes under NFκB control using the ribonuclease protection assay (RPA). We did perform this as shown in Figure 6 . As one can see, bFGF and VEGF increase TRAF-1 and this is decreased with parthenolide. We confirmed these findings with a Southern blot analysis.

Fig 6

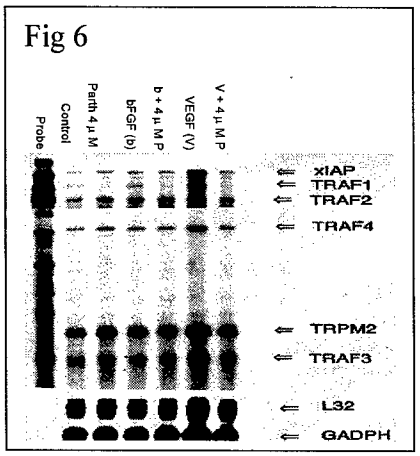


Figure 7: TRAF-1

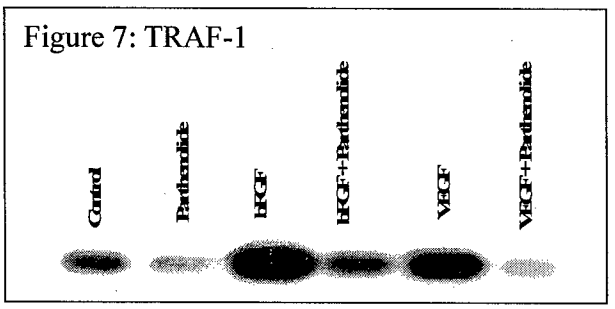


To study other genes we have again also opted to perform the evaluation using a NFκB Superarray instead of the RPA as it assesses more genes under NFκB control.

**Table 2. Effect of Parthenolide on gene expression profiles in HUVEC cells.**

| **Profile of Gene's down regulated** | **Gene name** | **Percent Change** |
|---|---|---|
| Homo sapiens B-factor, properdin (BF), | B-factor | 43.56 |
| Homo sapiens interferon, alpha 1 (IFNA1) | IFNA1 | 52.05 |
| Interleukin 12B,p40 | IL-12B | 74.4 |
| Interleukin 1, alpha | IL-1a | 69.96 |
| Serum amyloid A1 | SAA1 | 86.95 |
| Human endothelial leukocyte adhesion molecule I | ELAM-1/E-selectin | 46.81 |
| Human P-selectin glycoprotein ligand (SELPLG) | P-selectin | 78.46 |
| Homo sapiens toll-like receptor 5 (TLR5), | TLR5 | 53.14 |
| Homo sapiens toll-like receptor 6 (TLR6) | TLR6 | 36.29 |
| TNF receptor-associated factor 1 | TRAF1 | 38.38 |
| TNF receptor-associated factor 2 | TRAF2 | 41 |
| Vascular cell adhesion molecule 1 | VCAM-1 | 60.58 |
| **Profile of Gene's Up regulated** | | |
| p38 mitogen activated protein (MAP) kinase | p38 MAPK | 242.8 |
| Protein kinase mitogen-activated 8 (MAP kinase) | JNK1 | 380.9 |
| Protein kinase mitogen-activated 9 (MAP kinase) | JNK2 | 847.7 |
| Homo sapiens TNF receptor-1 associated protein | TRADD | 663.2 |

*d. Correlate the level of gene expression with changes in the corresponding protein.*

We again opted to evaluate the effect of parthenolide on TRAF-1 and TRAF-2 levels. The results confirmed the findings from the RPA. Specifically, bFGF and VEGF increase the levels of these anti-apoptotic cytokines and this can be abrogated by parthenolide. These findings are consistent with the known cell survival functions of these cytokines.

Figure 8a and 8b

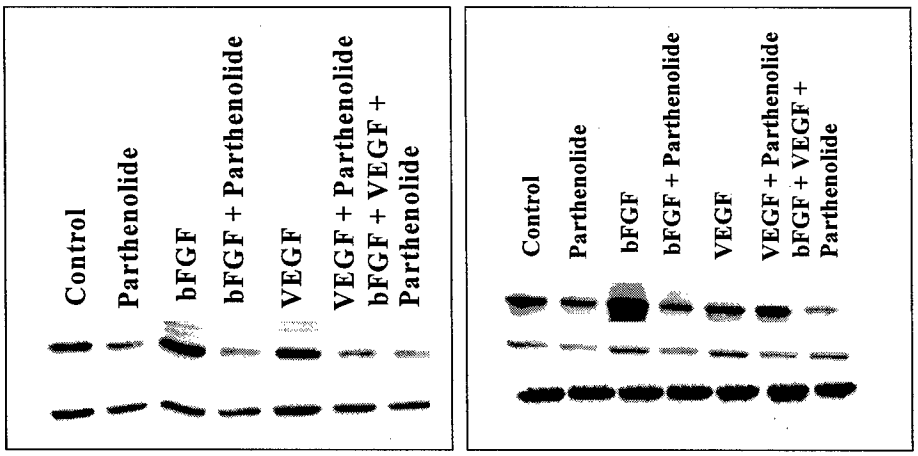


**Task 3. Evaluate the anti-cancer properties of parthenolide.**

*a). Perform in vitro cell proliferation assays of parthenolide in LNCaP, C4-2 and HUVECs as a single agent in combination with docetaxel and 2-methoxyestradiol and charcoal stripped serum.*

Figure 9

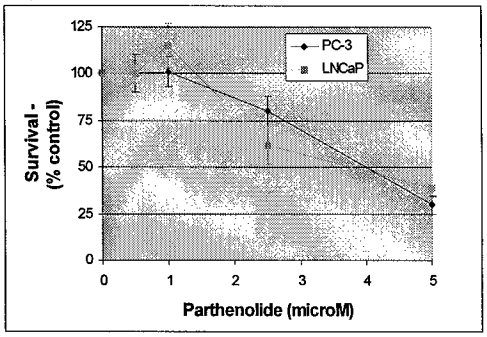


Figure 10 (CWR22Rv1)

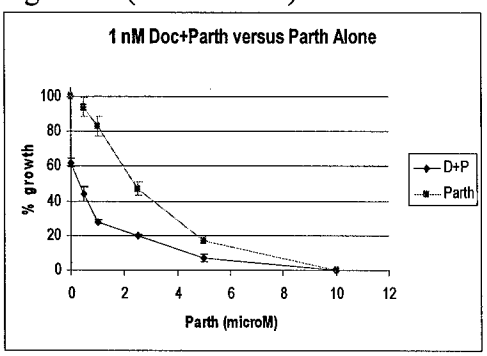


We have shown that parthenolide is able to decrease prostate cancer cell growth *in vitro*. Figure 9 shows the results of an MTS-PMS assay of LNCaP and PC-3. In the original grant application we proposed to evaluate LNCaP and C42 in the combinations described above. We subsequently had problems with the media for the C42 cell line and got unreliable results. We switched to the CWR22Rv1 cell line for the experiments. To assess the expansion of cell number in this cell line we performed clonogenic assays as it was not reliably assessed with the MTT-PMS assay. This change also complimented the *in vivo* work described below as this cell line has been growing reliably in both the *in vitro* and *in vivo* settings. As shown in Figure 10 we have shown that parthenolide significantly increases the cytotoxic effectiveness of docetaxel with 5 nM docetaxel alone decreasing the formation of clones by 40% and parthenolide at 1 μM decreased clone formation by only 20% however, the combination at these doses decreased the number of clones by 75%. Our previous report has detailed that parthenolide is able to decrease HUVEC proliferation with an IC50 of 7.5 μM and capillary formation with an IC50 of 4 μM. When using the Chou and Talalay assessment for synergy, this was observed. However, the combination decreased clone formation by 75%. The "Calcusyn" program demonstrated synergy. The combination indices (CI) for each micromolar dose of parthenolide (P) with 5nM of docetaxel were – 0.5P-CI: 0.87; 1P-CI: 1.07; 2.5P-CI: 0.89; 5P-CI: 0.41. A CI of 0.9 to 1.10 indicates additivity and 0.85-0.90 slight synergy and 0.7 to 0.85 moderate synergy and 0.3 to 0.7 strong synergy.

*b. Perform in vivo experiments with 20 mice in each cohort of parthenolide, docetaxel, 2-methoxyestradiol and parthenolide + docetaxel and parthenolide + 2 methoxyestradiol and parthenolide + castration..*

To facilitate translation of our *in vitro* findings into representative animal models, we determined the plasma concentration of parthenolide in mice following a two week dosing regimen. Parthenolide was administered via oral gavage at dose ranges from 0.4 up to 40 mg/kg/day. One hour post-gavage, we measured plasma concentrations of 112 nM at the 4mg/kg dose and 170 nM at the 40mg/kg dose. Parthenolide is a very lipophilic molecule and studies have shown that the systemic concentration can underestimate the cellular concentration of such lipophilic drugs[14,15]. However, no overt acute toxicity was evident in any of the animals and we therefore pursued the 40 mg/kg/day dose regimen in the following *in vivo* tumor models.

Of common concern to all cancer investigators is the difficulty in relating the available tumor models to the human disease. Therefore, we selected a model based on its clinical relevance and resistance to chemotherapy and hormonal therapy. Hence we used the human derived androgen resistant cell line, CWR22Rv1 in the flank of the subcutaneous tissue of male mice[16]. We initially performed experiments with C-42 implanted into the tibia of male mice, however, we were not able to measure tumor volume reliably and we switched to CWR22Rv1 in the flank.

We subsequently assessed the activity of parthenolide with both docetaxel and the anti-androgen, bicalutamide. Docetaxel was chosen as a point of reference since it is one of the most active drugs in the clinic for prostate cancer. Bicalutamide was chosen with the intent of determining whether parthenolide could restore some degree of sensitivity to hormonal therapy to this cell line that grows in castrate mice. It also needs to be pointed out that therapy was started 14 days after tumor implantation so the tumors would be established and undergoing exponential growth. This is a more "rigorous" model rather than commencing therapy when the tumors are only starting to adapt to their new environment and better represents the clinical setting of macroscopic metastatic disease. As such if activity is observed, we would have a more reliable read-out.

Parthenolide with weekly docetaxel in a prostate cancer heterotopic model: The treatment schedule employed was: 1) 40 mg/kg of parthenolide per day in 100 μL of 13% alcohol via oral gavage, 2) 5 mg/kg of intraperitoneal (i.p.) docetaxel in 13% alcohol weekly or, 3) the combination of docetaxel and parthenolide. Appropriate vehicle controls were used (oral daily and i.p. weekly). To extend the above findings beyond one cancer cell line and tumor type, we established mice bearing the hormone independent prostate cancer cell line CWR22Rv1 in their flanks. Treatment was commenced two weeks after implantation when the tumors were about 20 $mm^3$. After three weeks of treatment parthenolide and docetaxel as single agents both suppressed tumor growth by 15% and the combination of docetaxel plus parthenolide decreased growth by 55% compared with control (P = 0.01) (Figure 11). The number of mice alive by day 43 decreased because the veterinarians declared the mice with large necrosing tumors were to be sacrificed. The number sacrificed were: control group 7 of 22; parthenolide alone group 3 of 20; docetaxel alone group 5 of 20 and in the combination 1 of 22 had needed to be sacrificed. A linear growth curve model was fit using a mixed model with a variance-covariance model that incorporates

Figure 11:

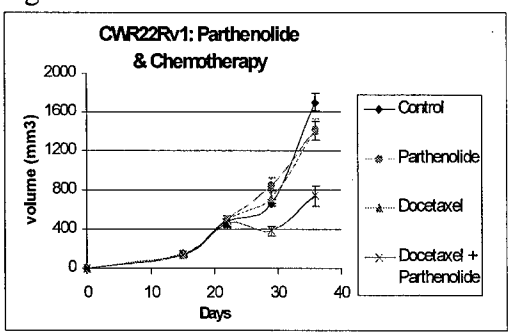

correlations of observations across time was also constructed. The rate of change of tumor volume between treatment groups was evaluated by comparing the slope estimates from the model. Data for this analysis was only taken out to day 22 of therapy because of the "drop-outs" from mice needing to be sacrificed. The rate of change for the docetaxel + parthenolide versus control was -43.11 (p=0.0009), and was also statistically less than docetaxel alone (p=0.016) and parthenolide alone (p=0.011). The rate of change for docetaxel versus control was -11.1 (p=0.40) and parthenolide versus control was -9.7 (p=0.45).

Small animal PET imaging using [$^{11}$C]CO and [$^{18}$F]choline (FCH) was performed on a random subset of four mice from each group to assess *in vivo* blood volume and choline metabolism (cell membrane proliferation), respectively. The relative blood volume, expressed as the ratio of tumor surface to muscle [$^{11}$C]CO concentrations, was 1.31±0.73 for solvent control; 1.27±0.86 for parthenolide; 1.19±0.29 for docetaxel and 0.50±0.13 for the combination (combination vs. solvent control p = 0.04). FCH uptake was also significantly decreased in the combination group (control=1.15±0.10; D+P=0.74±0.24, p=0.05).

Interestingly, docetaxel, despite being at the forefront of current therapy for prostate cancer, is ineffective as a single agent in this animal model at this dose and schedule. The highly significant augmentation in docetaxel's efficacy when combined with parthenolide in the robust prostate cancer model utilized in these studies is a very exciting result and illustrates the promise of this novel pro-apoptotic molecule.

Parthenolide with bicalutamide in an andogen independent prostate cancer heterotopic model:

To assess the ability to restore sensitivity to hormonal therapy we employed the same model as described for the parthenolide plus docetaxel. In this experiment, docetaxel was substituted with the anti-androgen bicalutamide at 50 mg/kg. This dose was shown to be the maximally effective dose in one of the hormonally sensitive derivatives of CWR22, (ie CWR22LD). After 21 days of therapy we observed that parthenolide can restore sensitivity to hormonal therapy as there is no inhibition with bicalutamide and with parthenolide after 14 and 21 days of therapy there was a 16% and 0% inhibition of growth respectively (ie minimal to no activity). However, the combination of bicalutamide plus parthenolide after 14 and 21 days resulted in 57% and 45% inhibition respectively. Statistical analyses will be done as described above.

Figure 12:

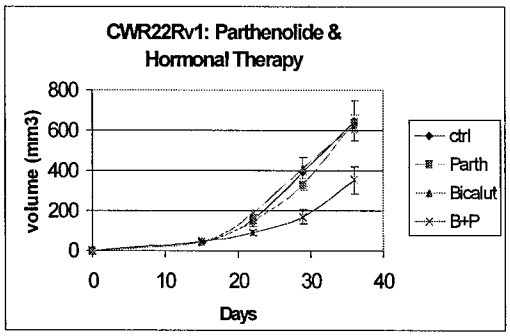


Using the C4-2 cell line in the tibia and measuring PSA six weeks, treatments were commenced and continued until week 10. The results of the serum PSA test are as follows:

| Treatment | N | Average PSA (ng/mL) | SE | Number of mice with detectable PSA |
|---|---|---|---|---|
| Parthenolide | 13 | 15.764 | 8.395 | 3 |
| Parthenolide and Docetaxel | 12 | 0 | 0 | 0 |
| Control | 16 | 4.756 | 2.595 | 4 |
| Docetaxel | 13 | 5.805 | 3.381 | 3 |

We saw that parthenolide had no effect as a single agent but was not different from docetaxel. The combination of parthenolide plus docetaxel had a profound effect with no mice having PSA at the time of sacrifice. The volumes of the tumors in the tibia were not measurable. This is another model that supports the data described above.

Finally our *in vivo* angiogenesis assay has shown parthenolide can decrease bFGF induced angiogenesis.

| | **VEGF** OD - SE (%Inhibition) | **bFGF** OD - SE **(%Inhibition)** | **Plasma Parthenolide concentration 1 hr after oral gavage** |
|---|---|---|---|
| **Control** | 4.55 – 0.37<br>100% | 3.79 – 0.25<br>100% | 0 μM |
| **Parthenolide 0.4 mg/kg** | 3.89 - 0.23<br>14% (*P*=0.29) | 3.00 - 0.22<br>21% (*P*=0.07) | Undetectable |
| **Parthenolide 4 mg/kg** | 4.01 - .27<br>12% (*P* =0.46) | 2.26 – 0.24<br>41% (*P*=0.0002) | 0.112 μM |
| **Parthenolide 40 mg/kg** | 3.60 - 0.26<br>21% (*P* =0.09) | 2.08 – 0.30<br>45.3% (*P*<0.0001) | 0.169 μM |

**Immuno-histochemical (IHC) analysis of resected tumors.**

To evaluate the biological changes *in vivo* tumors were resected tumors when the mice were sacrificed and fixed the tumors in formalin and embedded them in paraffin and subjected them to IHC. Nuclear staining for phosphorylation of JNK in the nuclear staining of tumors from control mice showed a staining index of 1.2. The mice that received parthenolide alone had similar staining index of 1.3. While mice treated with docetaxel (2.1) or combination (2.3) showed a higher JNK staining. Microvessel density was also assessed to measure the amount of angiogenesis in the tumors. We discovered that the amount of vessel formation (expressed microvessels per high pwered field) in the presence of parthenolide was 22.5 (±13.6) versus 23.8 (±11.9) with docetaxel This was numerically but not statistically less that the results of 40.1 (±14.7) for the solvent control group. Significantly lower vessel density was observed in tumors of mice that received the combination with 15.3 (±6.9).

This data demonstrates the ability of parthenolide to impact both the cancerous and endothelial compartments of established xenograft when combined with a cytotoxic agent. The IHC data also demonstrated the ability of docetaxel at this dose and schedule to enhance JNK activation (phosphorylation) *in vivo* but was not enough to slow tumor growth. In contrast the combination of docetaxel plus parthenolide was able to slow tumor growth. This would suggest that in this xenograft model the ability to activate JNK is not enough to induce an anticancer effect. At this dose and schedule parthenolide did not augment the intensity of nuclear JNK phosphorylation. Thus, it is to be speculated that parthenolide altered a second pathway and promoted the anti-cancer acitivity. Our attempts to measure NFκB DNA binding by EMSA and IHC yielded inconclusive results due to (i) lack of a reliable IHC antibody to measure NFκB DNA binding by staining for the p65 subunit and (ii) the EMSA results being confounded by the data being an analysis of the necrotic tumor rather than the cancer cells themselves. Work to define the relative contribution of parthenolide's ability to inhibit NFκB DNA binding and/or activate JNK to its anti-cancer and anti-angiogenic properties is ongoing. Other work required to be done is determine the pathways that are altered by parthenolide and restore sensitivity to bicalutamide

Due to the efforts required to perform the C42 tibial model and replacing with the CWR22RV1 we were not able to complete the work with 2ME2.

**This task was completed with slight modifications to the original plan.**

**Task 4. Evaluate the clinical relevance of NFκB activation.**

*a. Access paraffin embedded tissue from the pathology department of Indiana university Medical Center and stain for the p65 subunit and correlate with clinical outcome(Months 33 to 36).*

*Clinicopathological Experiments:*

Ninety seven cases of radical prostatectomy were analyzed by immunohistochemistry. The antibody employed was a rabbit polyclonal antibody that identifies the binding site of the p65 subunit of the Rel family. (Santa Cruz Biotechnology, Santa Cruz, CA). Serial 5-μm-thick sections of formalin-fixed slices of radical prostatectomy specimens were used for the studies. The tissue blocks containing the highest Gleason score and the maximum amount of tumor were selected. Immunoreactivity for the p65 subunit was seen in 90%, 99% and 100% of all the specimens. However, the amount of immunoreactivty was greater in the neoplastic lesions compared with the benign glands. Specifically, the mean percent staining intensity was 14.7% in the benign glands and 79.2% in PIN and 88.7% in the adenocarcinoma. The difference in amount of staining was significantly greater in the PIN lesions compared with the benign glands ($p < 0.001$) and was greater in the invasive neoplastic disease compared with the intraepithelial neoplasia ($p < 0.001$)

| Staining | Proportion p65 Present | Mean Staining (SD) | Range |
|---|---|---|---|
| Normal | 90% | 14.7% (17.1) | 0-50 |
| PIN | 99% | 79.2 (17.8) | 0-95 |
| Cancer | 100% | 88.7% (12.1) | 35-95 |

| Intensity | 0 | 1 | 2 | 3 |
|---|---|---|---|---|
| Normal | 9(9%) | 57(58%) | 31(32%) | 0(0%) |
| PIN | 1(1%) | 10(10%) | 62(64%) | 24(24%) |
| Cancer | 0(0%) | 0(0%) | 29(29%) | 68(70%) |

The differential staining (frequency and amount) and graded increase between the normal, PIN and cancerous areas supports the contention that staining for the IκB binding site on the p65 subunit does represent activated NFκB. The presence of staining in all the cancer specimens support the *in vitro* data that activated NFκB is a common finding. The low amount of nuclear staining is probably due to the very short half life of transcription factors in the nucleus. The lack of association between pathological and clinical prognostic features is secondary to the universal staining at either 2+ or 3+ intensity.

**This task has been completed.**

## KEY RESEARCH ACCOMPLISHMENTS

- NFκB DNA binding is present in all prostate cancer cells and is overexpressed in human prostatectomy specimens
- Parthenolide decreases NFκB DNA binding and many genes under its transcriptional control in both prostate cancer cells and endothelial cells.
- Parthenolide has single agent anti-cancer activity *in vitro* and can augment the efficacy of docetaxel
- *In vivo* parthenolide is able to restore hormone sensitivity to androgen resistant cell line despite suboptimal pharmacokinetic properties.
- Parthenolide has anti-angiogenic properties both *in vitro* and *in vivo*

## REPORTABLE OUTCOMES

Manuscripts:

- Sweeney C, Li L, Shanmugam R, et al: Nuclear factor-kappaB is constitutively activated in prostate cancer in vitro and is overexpressed in prostatic intraepithelial neoplasia and adenocarcinoma of the prostate. Clin Cancer Res 10:5501-7, 2004
- Shanmugan, R et al "Restoring chemotherapy and hormone therapy sensitivity by parthenolide in a xenograft hormone refractory prostate cancer model" manuscript in preparation which is to be submitted to Cancer Research June 2005.

Abstracts:

- Proceeding American Association for Cancer Research 2004
    - *"IN VIVO* ANTI-PROSTATE CANCER PROPERTIES OF PARTHENOLIDE CORRELATED WITH PET IMAGING"

Presentations:

- none

Patents and licenses applied for and/or issued:

- **Nakshatri; Harikrishna** and **Sweeney; Christopher J.** (Indianapolis, IN)
- **Patent number: 6,890,946**
- **Issued** May 10, 2005
- **Title:** Use of parthenolide to inhibit cancer

Funding applied for based on work supported by this award;

- Rapid access to intervention development RAID application
    - First application Feb 2005 was successful and defined the PK profile of parthenolide
    - Second application Feb 2006 for scale-up production under review and preparation for
- DOD Idea Award: A mechanistic evaluation of dimethlyaminoparthenolide's anti-cancer properties – submitted February 2005

**CONCLUSIONS:**

In this study, we have demonstrated the molecular effects of parthenolide on both an androgen independent prostate cancer cell line and endothelial cells. Specifically, we have documented that parthenolide blocks NFκB DNA binding in both cancerous and endolthelial cells and decreases the expression of anti-apoptotic genes (TRAF-1 and TRAF-2) under NFκB control. These molecular events were seen at doses of parthenolide (approximately 5 μM) that were also observed to inhibit clone formation of CWR22Rv1 as well as the ability of HUVECs to proliferate and form capillaries. Moreover, we clearly demonstrate the ability of parthenolide to enhance the ability of docetaxel to inhibit clonogenic formation *in vitro*.

However, further clinical development of parthenolide is confounded by data from our RAID application demonstrating the low bioavailability of parthenolide. Specifically, this work has demonstrated that the dose of parthenolide used in these *in vivo* experiments provides only low nanomolar concentrations of parthenolide to the bloodstream[17]. Moreover, this work demonstrated that higher doses would not increase the serum levels. As such water soluble analogues of parthenolide with the same type and amount of *in vitro activity* and provide plasma concentrations that exceed 10 μM have been developed[17]. Despite, this it is interesting to note that parthenolide still had some *in vivo* activity. This could be due to assessment of the systemic concentration of lipophilic molecules parthenolide may underestimate the cellular concentration of such drugs and this has been well described for nicotine[14,15].

In summary we have shown that parthenolide is a new anti-cancer agent with the unique property of inhibition of NFκB and associated decrease in anti-apoptotic proteins TRAF1, TRAF 2 in both cancer and endothelial cells. Activation of JNK was also observed. These changes were associated with inhibition of cell proliferation *in vitro* and restoration of CWR22Rv1 sensitivity to chemotherapy and bicalutimide. However, parthenolide is poorly bioavailable and water soluble analogues are being developed to overcome this problem which may result in single agent with anti-cancer activity *in vivo* through inhibition of NFκB and activation of JNK. This work is ongoing.

**REFERENCES**

1. Kwok BH, Koh B, Ndubuisi MI, et al: The anti-inflammatory natural product parthenolide from the medicinal herb Feverfew directly binds to and inhibits IkappaB kinase. Chem Biol 8:759-66, 2001

2. Hehner SP, Hofmann TG, Droge W, et al: The antiinflammatory sesquiterpene lactone parthenolide inhibits NF-kappa B by targeting the I kappa B kinase complex. J Immunol 163:5617-23, 1999

3. Mendonca M, Hardacre, M, Datzman, N, Comerford, K, Chin-Sinex, H, Sweeney C.: Inhibition of constitutive NFkappaB activity by the anti-inflammatory sesquiterpene, parthenolide slows cell growth and increases radiation sensitivity. Int J Radiat Oncol Biol Phys. 57::S354, 2003

4. Nozaki S, Sledge Jr GW, Nakshatri H: Repression of GADD153/CHOP by NF-kappaB: a possible cellular defense against endoplasmic reticulum stress-induced cell death. Oncogene 20:2178-85., 2001

5. Baeuerle PA, Henkel T: Function and activation of NF-kappa B in the immune system. Annu Rev Immunol 12:141-79, 1994

6. Helbig G, Christopherson KW, 2nd, Bhat-Nakshatri P, et al: NF-kappaB promotes breast cancer cell migration and metastasis by inducing the expression of the chemokine receptor CXCR4. J Biol Chem 278:21631-8, 2003

Sweeney, Final Report; DAMD17-02-1-1-0072

7. Jones PL, Ping D, Boss JM: Tumor necrosis factor alpha and interleukin-1beta regulate the murine manganese superoxide dismutase gene through a complex intronic enhancer involving C/EBP-beta and NF-kappaB. Mol Cell Biol 17:6970-81, 1997

8. Zong WX, Edelstein LC, Chen C, et al: The prosurvival Bcl-2 homolog Bfl-1/A1 is a direct transcriptional target of NF-kappaB that blocks TNFalpha-induced apoptosis. Genes Dev 13:382-7., 1999

9. Lee HH, Dadgostar H, Cheng Q, et al: NF-kappaB-mediated up-regulation of Bcl-x and Bfl-1/A1 is required for CD40 survival signaling in B lymphocytes. Proc Natl Acad Sci U S A 96:9136-41., 1999

10. Baldini N: Multidrug resistance--a multiplex phenomenon. Nat Med 3:378-80, 1997

11. Wang CY, Mayo MW, Baldwin AS, Jr.: TNF- and cancer therapy-induced apoptosis: potentiation by inhibition of NF-kappaB. Science 274:784-7., 1996

12. Pahl HL: Activators and target genes of Rel/NF-kappaB transcription factors. Oncogene 18:6853-66, 1999

13. Hanahan D, Weinberg RA: The hallmarks of cancer. Cell 100:57-70, 2000

14. Ghosheh OA, Dwoskin LP, Miller DK, et al: Accumulation of nicotine and its metabolites in rat brain after intermittent or continuous peripheral administration of [2'-(14)C]nicotine. Drug Metab Dispos 29:645-51, 2001

15. Ghosheh O, Dwoskin LP, Li WK, et al: Residence times and half-lives of nicotine metabolites in rat brain after acute peripheral administration of [2'-(14)C]nicotine. Drug Metab Dispos 27:1448-55, 1999

16. Sramkoski RM, Pretlow TG, 2nd, Giaconia JM, et al: A new human prostate carcinoma cell line, 22Rv1. In Vitro Cell Dev Biol Anim 35:403-9, 1999

17. Cheng D, Xiao JJ, Cheng H, et al: Analytical method development and pharmacokinetics studies with parthenolide (NSC 157035) and a water-soluble analog (NSC 734325). Proc Am Assoc Canc Res 46:4184 (abstr), 2005

## APPENDICES

**Clinical Cancer Research manuscript.**

# Nuclear Factor-κB Is Constitutively Activated in Prostate Cancer *In vitro* and Is Overexpressed in Prostatic Intraepithelial Neoplasia and Adenocarcinoma of the Prostate

**Christopher Sweeney,[1] Lang Li,[2] Rajasubramaniam Shanmugam,[1] Poornima Bhat-Nakshatri,[8] Vetrichelvan Jayaprakasan,[1] Lee Ann Baldridge,[5] Thomas Gardner,[3] Martin Smith,[4] Harikrishna Nakshatri,[6] and Liang Cheng[5,7]**

Departments of [1]Medicine, [2]Biostatistics, [3]Urology, [4]Microbiology and Immunology, [5]Pathology, and [6]Surgery, Indiana University, Indianapolis, Indiana; [7]Department of Pathology, Roudebush Veterans Affairs Medical Center, Indianapolis, Indiana; and [8]Walther Cancer Institute, Indianapolis, Indiana

## ABSTRACT

***Purpose:*** **The transcription factor nuclear factor-κB (NF-κB) promotes the production of angiogenic, antiapoptotic, and prometastatic factors that are involved in carcinogenesis.**

***Experimental Design:*** **Electromobility gel shift assays were used to evaluate NF-κB DNA binding *in vitro*. The functional relevance of NF-κB DNA binding was assessed by both cDNA array analyses and proliferation assays of prostate cancer cells with and without exposure to an NF-κB inhibitor, parthenolide. Immunohistochemistry staining for the p65 NF-κB subunit was used to determine the frequency and location of NF-κB in 97 prostatectomy specimens. The amount of staining was quantified on a 0–3+ scale.**

***Results:*** **An electromobility gel shift assay confirmed the presence of NFκB DNA binding in all four prostate cancer cell lines tested. The binding was inhibited by parthenolide, and this agent also decreased multiple gene transcripts under the control of NF-κB and inhibited proliferation of prostate cancer cells. The staining results revealed overexpression of p65 in the prostatic intraepithelial neoplasia and cancer compared with the benign epithelium. Specifically, there was a predominance of 1+ and 2+ with no 3+ staining in benign epithelium, whereas there was only 2+ and 3+ staining (30 and 70%, respectively) in the cancerous areas. These differences were statistically different. There was no correlation with tumor grade or stage.**

***Conclusions:*** **NF-κB is constitutively activated in prostate cancer and functionally relevant *in vitro*. Immunohistochemistry of human prostatectomy specimens demonstrated overexpression of the active subunit of NF-κB, p65, and that this occurs at an early stage in the genesis of prostate cancer. This work supports the rationale for targeting NF-κB for the prevention and/or treatment of prostate cancer.**

## INTRODUCTION

Nuclear factor-κB (NF-κB) is a dimeric transcription factor composed of members of the Rel family (1). The predominant NF-κB dimers are the transcriptionally active p65:p50 heterodimer and the less active p50:p50 homodimer (2). NF-κB dimers are bound to inhibitory IκB proteins in the cytoplasm and released from inhibitor of nuclear factor-κB (IκB) after phosphorylation of IκB by Iκ kinases followed by proteosome-mediated degradation of IκB. The release of NF-κB and subsequent binding to DNA occurs in response to a variety of stimuli, including chemotherapy, radiation, and cytokines such as tumor necrosis factor α (TNF-α) and interleukin (IL)-1. Genes activated by NF-κB play a central role in many of the hallmarks of prostate cancer, including invasion (IL-6 and matrix metalloproteinase 9), angiogenesis (IL-8, vascular endothelial growth factor), and inhibition of apoptosis (cIAP 1, c-IAP 2, TRAF-1, TRAF-2, Bfl-1/A1, Bcl-$X_L$, and manganese superoxide dismutase; Refs. 3–6).

Induction of NF-κB promotes resistance to TNF and chemotherapy (6) and inhibition of NF-κB activation by overexpression of IκB restores chemotherapy and TNF sensitivity. This suggests that constitutive NF-κB activation may be an important mechanism of hormonal and chemotherapy resistance. Studies of cell lines *in vitro* have shown that NF-κB is constitutively activated in many malignancies, including breast cancer and prostate cancer (7, 8). Recently, investigators have shown that inhibition of NF-κB by insertion of mutated IκB into cancer cell lines causes decreased vascular endothelial growth factor and IL-8 expression and was associated with decreased *in vivo* growth with decreased angiogenesis of an ovarian cancer cell line (9, 10). Emerging preclinical evidence implicates NF-κB in the development of prostate cancer because it has been shown to regulate bcl-2 transcription (8) and inhibition of NF-κB results in apoptosis (11) and cell cycle arrest (12).

Therapy directed against the transcription factor NF-κB is therefore a prime target and has the potential to improve the prognosis of prostate cancer patients. This latter point is underscored by findings from the clinical trials of the proteasome inhibitor PS 341. This drug blocks NF-κB (in addition to other pathways) and induces remissions and suppression of proteins under NF-κB control (*e.g.*, IL-6) in patients with multiple my-

Received 4/15/03; revised 4/29/04; accepted 5/10/04.

**Grant support:** Department of Defense Grant DAMD17-02-1-1-0072, American Institute Cancer Research Grant OOA047, and the Walther Cancer Institute.

The costs of publication of this article were defrayed in part by the payment of page charges. This article must therefore be hereby marked *advertisement* in accordance with 18 U.S.C. Section 1734 solely to indicate this fact.

**Requests for reprints:** Christopher Sweeney, Indiana University, Room 473, 535 Barnhill Drive, Indianapolis, IN 46202. Phone: (317) 274-3515; Fax: (317) 274-3646; E-mail: chsweene@iupui.edu.

eloma, hormone refractory prostate cancer, and non-small cell lung cancer (13, 14).

Electromobility gel shift analyses were undertaken to confirm the presence of NF-κB DNA binding *in vitro* in a variety of prostate cancer cells lines and to determine whether this could be inhibited by the NF-κB inhibitor parthenolide. The functional relevance of NF-κB DNA binding was assessed by cDNA array analyses and proliferation assays of prostate cancer cells with and without exposure to a NF-κB inhibitor, parthenolide. The immunohistochemistry analysis was undertaken to determine the frequency and location of NF-κB by staining for the p65 subunit of the Rel family.

## MATERIALS AND METHODS

**Electromobility Gel Shift Assay.** All prostate cancer cells were plated on 100-mm plates and harvested in exponential growth phase. The prostate cancer cells were (*a*) the hormone-sensitive cell line LNCaP (in three different passage states: low passage, 11 passages; intermediate passage, 38 passages; and high passage, 208 passages); (*b*) PC-3 (hormone-independent cell line) and (*c*) C42 (a hormone-independent subclone of LNCaP). The LNCaP P-11 and 208 and PC-3 cells were cultured in MEM with 10% fetal bovine serum and were obtained from American Type Culture Collection (Manassas, VA). The LNCaP P-38, the parental clone of the C42 cells, and the C42 cells were provided by Dr. Thomas Gardner and cultured in T-media (Life Technologies, Inc., Rockville MD). The CWR22Rv1 cell line was kindly provided by Dr. James Jacobberger (15). The cells were grown in DMEM containing 10% FCS.

Solvent control and parthenolide dissolved in 100% ethanol (Aldrich, Milwaukee WI) were added 3 h before harvesting. Whole cell extracts were prepared as previously described (7) and incubated with a radiolabeled NF-κB probe for 30 min at room temperature. The oligonucleotide probe binds to the NF-κB DNA binding site in the promoter region of the immunoglobulin gene. Electrophoresis and autoradioragraphy were performed as previously described (7) using NF-κB and SP-1 probes (Promega, Madison, WI). The specificity of parthenolide inhibiting NF-κB DNA binding was verified by the use of the SP-1 probe as a control.

**cDNA Array Analysis.** Total cellular RNA was extracted from CWR22Rv1 after 6 h of exposure to solvent control and 10 μmol/liter parthenolide using RNeasy Minikit (Quiagen, Valencia, CA) according to the manufacturer's instructions. The NF-κB pathway GE array kit was obtained from SuperArray Bioscience Corp. (Bethesda, MD). The kit determines expression of 96 genes that either interact with or are controlled by NF-κB. Total RNA from respective samples were used as a template to generate biotin-labeled cDNA probes using GEArray Ampolabelling RT kit (SuperArray Bioscience Corp.). The cDNA probes corresponding to the mRNA population were then denatured, and hybridization was carried out in GEHyb solution to nylon membranes spotted with gene-specific fragments. Membranes were then washed in 2× SSC, 1% SDS twice for 15 min each, followed by 0.1× SSC, 0.5% SDS twice for 15 min each. Chemiluminescence was used to visualize the expression levels of each transcript, and the results were quantified with the GEArray Analyzer. The change in a given gene transcript was estimated by normalizing the signal intensities with the signals derived from glyceraldehyde-3-phosphate dehydrogenase and β-actin.

**Proliferation Assay.** LNCaP and PC-3 cells were plated in a 96-well U-bottomed plate (Becton Dickinson Labware, Franklin Lakes, NJ) at a concentration of 5000 cells/50 μl media and incubated in 5% $CO_2$ at 37°C for 24 h. Varying parthenolide concentrations in 50 μl of media were added to the media 24 h later. Colorimetric readings were obtained using the Cell Titer 96 $AQ_{ueous}$ Non-radioactive Cell Proliferation Assay (Promega Corp.; Madison, WI) system and an ELISA plate reader after 48 h of exposure to parthenolide. The readings obtained for each concentration tested were from an average of eight wells. Each experiment was expressed as a percentage of the solvent control and completed at least three times with consistent results. The results presented are an average of three experiments.

**Tissue Samples.** Ninety-seven cases of radical prostatectomy and bilateral lymphadenectomy between 1990 and 1994 were obtained from the surgical pathology files of Indiana University Medical Center. Institutional Review Board approval was obtained from the Indiana University Purdue University Institutional Review Board. Complete clinical and pathological data were available for 93 patients. Patients ranged in age from 51 to 78 years (mean, 63 years). Grading of the primary tumor from the radical prostatectomy specimens was performed according to the Gleason's system. The Gleason grade ranged from 4 to 10. Pathological stage was performed according to the 1997 Tumor-Node-Metastasis system. Pathological stages were as follows: $T_{2a}$ ($n$ = 12 patients); $T_{2b}$ ($n$ = 42 patients), $T_{3a}$ ($n$ = 25 patients, and $T_{3b}$ ($n$ = 14 patients; Table 1). Thirteen (14%) patients had lymph node metastasis at the time of surgery. Clinical and complete pathological data were not available for four patients.

**Immunohistochemical Studies.** The antibody used was a rabbit polyclonal antibody that identifies the $NH_2$-terminal domain of NF-κB p65 of human origin (SC 109; Santa Cruz Biotechnology, Santa Cruz, CA). Serial 5-μm thick sections of formalin-fixed slices of radical prostatectomy specimens were used for the studies. The tissue blocks containing the highest Gleason score and the maximum amount of tumor were selected. One representative slide from each case was analyzed, and we recognized the limitation of sample variation. Samples were removed from the paraffin by placing them three times in xylene for 5 min and then rehydrating through graded ethanol and finally immersion in distilled water. Slides were then rinsed in Tris-buffered saline. Antigen retrieval was performed by using the Dako Target Retrieval kit (Dako, Carpinteria, CA) containing a citrate buffer (pH 6.0) for 20 min at ~95°C. Dako's Avidin Biotin blocking system was used for 10 min, and the tissue sections were then rinsed with Tris-buffered saline. The nonspecific binding sites were blocked by incubating with Dako's Protein Block for 20 min. Tissue sections were then incubated with the polyclonal rabbit antibody against p65 (1:100 dilution at room temperature for 60 min). After washing with Tris-buffered saline, the secondary antibody, Dako Link (Dako LSAB2 kit) was applied for 20 min and then rinsed with Tris-buffered saline. Additional washing was followed by incu-

*Table 1* Patient characteristics

| $N = 93$ (data on four patients not available) | % of total patients ($N = 93$)* | Mean % of cells staining with p65 subunit of NF-κB antibody (± SD) | Mean p65 subunit of NF-κB antibody staining 0–3 (± SD) |
|---|---|---|---|
| Primary Gleason grade | | | |
| 2 | 14 | 83.0 ± 15.7 | 2.69 ± 0.48 |
| 3 | 46 | 88.9 ± 5.07 | 2.67 ± 0.47 |
| 4 | 27 | 90.4 ± 5.38 | 2.64 ± 0.49 |
| 5 | 13 | 89.6 ± 6.56 | 2.91 ± 0.29 |
| Secondary Gleason grade | | | |
| 2 | 16 | 87.3 ± 6.51 | 2.53 ± 0.52 |
| 3 | 37 | 89.1 ± 10.4 | 2.73 ± 0.45 |
| 4 | 34 | 88.6 ± 5.99 | 2.75 ± 0.44 |
| 5 | 13 | 88.8 ± 6.1 | 2.67 ± 0.49 |
| Gleason sum | | | |
| <7 | 32 | 85.8 ± 11.0 | 2.60 ± 0.49 |
| 7 | 42 | 90.38 ± 5.05 | 2.71 ± 0.46 |
| >7 | 26 | 89.1 ± 6.20 | 2.79 ± 0.41 |
| T classification | | | |
| $T_{2a}$ | 13 | 82.9 ± 16.6 | 2.75 ± 0.45 |
| $T_{2b}$ | 45 | 89.4 ± 4.71 | 2.64 ± 0.49 |
| $T_{3a}$ | 27 | 89.4 ± 6.00 | 2.60 ± 0.50 |
| $T_{3b}$ | 15 | 89.6 ± 6.03 | 3.0 ± 0.00 |
| Lymph node metastasis | | | |
| Positive | 13 | 90.4 ± 5.82 | 2.75 ± 5.82 |
| Negative | 87 | 88.3 ± 8.18 | 2.68 ± 0.47 |
| Extraprostatic extension | | | |
| Positive | 41 | 89.7 ± 5.80 | 2.73 ± 0.45 |
| Negative | 59 | 87.8 ± 9.01 | 2.67 ± 0.47 |
| Surgical margin | | | |
| Positive | 40 | 89.2 ± 5.46 | 2.78 ± 0.42 |
| Negative | 60 | 88.2 ± 9.16 | 2.64 ± 0.48 |
| Vascular invasion | | | |
| Positive | 27 | 90.6 ± 5.27 | 2.68 ± 0.48 |
| Negative | 73 | 87.9 ± 8.56 | 2.71 ± 0.46 |
| Perineural invasion | | | |
| Positive | 85 | 90.0 ± 8.02 | 2.7 ± 0.46 |
| Negative | 15 | 86.4 ± 6.91 | 2.64 ± 0.50 |
| High-grade PIN | | | |
| Positive | 98 | 88.7 ± 7.83 | 2.71 ± 0.45 |
| Negative | 2 | 82.5 ± 10.6 | 2.0 ± 0 |

* Data on 4 patients not available.

bation with streptavidin horseradish peroxidase (Dako Label, LSAB2 kit) for 20 min. Immunoreactivity was visualized by incubation of sections with 3,3′-diaminobenzidine in the presence of hydrogen peroxide. Sections were counterstained with light hematoxylin and mounted with a coverslip. All of the procedures were performed at room temperature.

The extent and intensity of staining were evaluated by a single pathologist (L. Cheng) in benign epithelium, prostate intraepithelial neoplasia (PIN), and adenocarcinoma from the same slide for each case. Microscopic fields evaluated and scored were those with the highest degree of immunoreactivity. A numeric intensity score of between 0 and 3 was assigned to each case on a scale of from 0 to 3 (0, no staining; 1+, weak staining; 2+, moderate staining; and 3+, strong staining). Inter- and intraobserver variation of staining was not assessed in the current study. The authors recognized the limitation and inherent subjectivity of immunostaining evaluation. A representative slide with 3+ staining is presented in Fig. 4.

**Statistical Analysis.** The intensity of staining in benign epithelium, PIN, and adenocarcinoma were compared using the Cochran-Mantel-Haenszel tests for correlated ordered categorical outcomes. Pairwise comparisons between the tissue types were made if the ANOVA revealed significant treatment effects. $P < 0.05$ was considered significant, and all $P$ values were two-sided.

## RESULTS

**Electromobility Gel Shift Analysis.** We have found *in vitro* that NF-κB DNA binding is present in all prostate cancer cell lines evaluated (Fig. 1). The proportion of the p65:p50 heterodimer to p50:p50 homodimer is lowest in the LNCaP cell lines that have undergone the least number of passages in culture compared with (*a*) the LNCaP cell lines that have undergone a higher number of passages and (*b*) the hormone independent cell lines—C42 and PC-3 (Fig. 1*A*). Also of note is that parthenolide is able to inhibit the NF-κB DNA binding in a dose-dependent manner starting at 0.5 μmol/liter. EMSA also showed that NF-κB DNA binding, present in the androgen-independent prostate cancer cell line CWR22Rv1 (Fig. 1*B*), and supershift assay on two occasions confirmed the presence of the active subunit p65 (data not shown). NF-κB DNA binding was again inhibited by parthenolide (Fig. 1*B*).

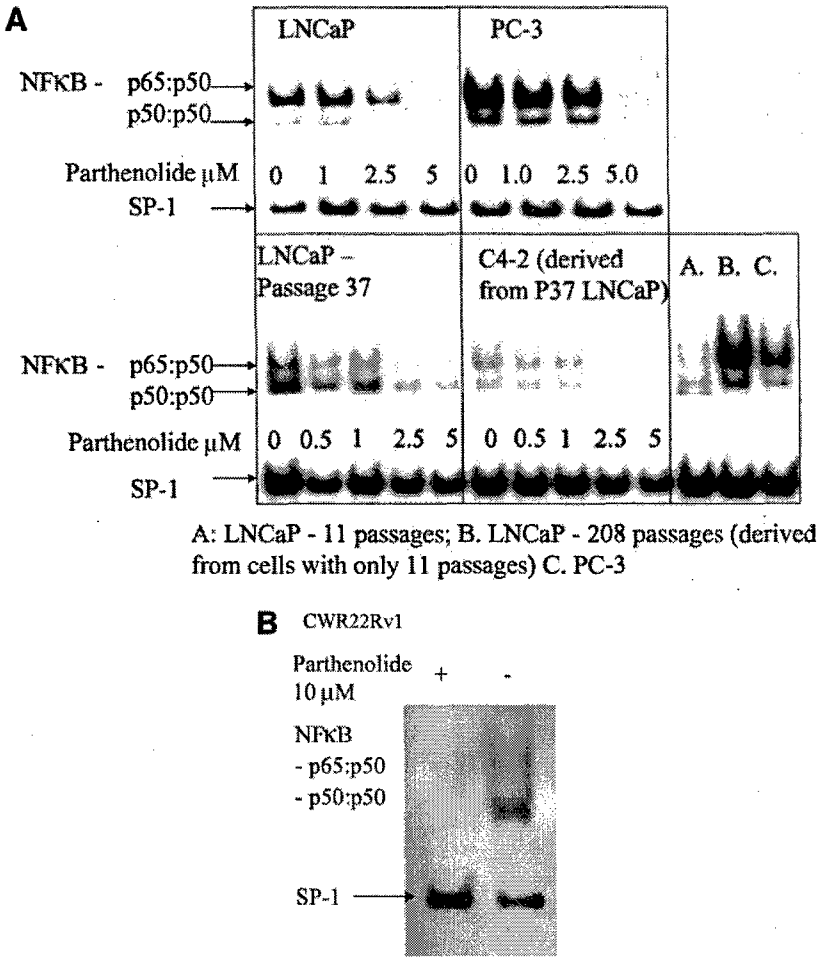


*Fig. 1 A*, electromobility gel shift assay showing that NF-κB DNA binding is present in all of the prostate cancer cells lines and that there is a greater proportion of p65:p50 compared with p50:p50 in cell lines that have undergone a greater number of passages and are hormone independent (PC-3 and C4-2). Parthenolide is able to inhibit the NF-κB DNA binding in a dose-dependent manner. (P-11, 11 passages; P-208, 208 passages; P-37, 37 passages). *B*, electromobility gel shift assay showing that NF-κB DNA binding is present in the androgen-dependent prostate cancer cell line, CWR22Rv1. The *first lane* shows loss of NF-κB DNA binding in the presence of 10 μmol/liter parthenolide. These results were confirmed with a repeat of the experiment.

**cDNA Array Analysis.** The relative expression level of 96 transcripts was determined using chemiluminescence and analyzed with GEArray Analyzer. All results were normalized by adjusting for the signal derived from glyceraldehyde-3-phosphate dehydrogenase and β-actin spots. The change in a given gene transcript from one membrane/experiment was estimated by comparing the signal intensities of paired specimens: parthenolide treated *versus* solvent control (Fig. 2). Genes that had at least a 10% decrease after 6 h of treatment compared with untreated control in two consecutive experiments were arbitrarily considered to show a magnitude and consistency in effect between experiments to support the hypothesis that genes under NF-κB control are present in prostate cancer cells and provide relevance to the electromobility gel shift findings. The 18 genes that met these criteria and have previously been shown to be under the transcriptional control of NF-κB (16) are detailed in Table 2. It is of note that genes associated with the hallmarks of cancer (17) were decreased with parthenolide treatment. Specifically, genes associated with evasion of apoptosis, TNF receptor associated factor-1 and TNF receptor associated factor-5, were decreased. Also, genes associated with maintaining cell-cell adhesion and thus preventing metastasis (intercellular adhesion

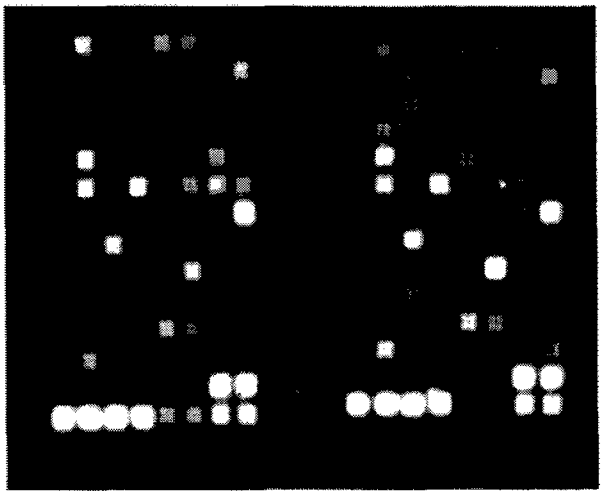


*Fig. 2* cDNA array of CWR22Rv1 cells with and without parthenolide. The panel on the left is an analysis of cells without treatment, and the panel on the right is after 6 h of exposure to parthenolide.

*Table 2* Genes under NF-κB control expressed in prostate cancer (CWR22Rv1) cells and decreased after treatment with the NF-κB inhibitor parthenolide.

| Gene | Experiment 1* | Experiment 2* | Average of 1 and 2* |
|---|---|---|---|
| Intercellular adhesion molecule 2 | 39 | 32 | 35.5 |
| Intercellular adhesion molecule 5, telencephalin | 47 | 80 | 63.5 |
| Interferon, α1 | 53 | 32 | 42.5 |
| IFN, β 1, fibroblast | 33 | 12 | 22.5 |
| IL-12β, p40 | 63 | 47 | 55 |
| IL-1, α | 75 | 13 | 44 |
| IL-1, β | 52 | 44 | 48 |
| IL-1 receptor type II | 16 | 44 | 30 |
| IL-1 receptor-associated kinase (IRAK) mRNA | 60 | 17 | 38.5 |
| Lymphotoxin-α (TNF superfamily, member 1) | 46 | 60 | 53 |
| Protein kinase, mitogen-activated 3 (MAP kinase 3; p44) | 43 | 40 | 41.5 |
| Neural cell adhesion molecule 1 | 35 | 57 | 46 |
| Orosomucoid 1 (ORM1, α-1 acid glycoprotein) | 53 | 51 | 52 |
| Transforming growth factor β-activated kinase-binding protein 1 (TAB1), | 17 | 50 | 33.5 |
| Toll-like receptor 10 (TLR10), | 20 | 80 | 50 |
| Tumor necrosis factor (TNF superfamily, member 2) | 46 | 28 | 37 |
| TNF receptor-associated factor 1 | 40 | 29 | 34.5 |
| TNF receptor-associated factor 5 | 20 | 13 | 16.5 |

* Results reported as percentage decrease of gene compared with untreated control cells.

molecule-2, ICAM-5) and genes associated with inflammation (TNF) were also decreased.

**Proliferation.** To assess if the inhibition of NF-κB in prostate cancer cells by parthenolide has antiproliferative properties we performed an Cell Titer 96 $Aq_{ueous}$ Non-Radioactive Cell Proliferation Assay (Promega Corp.) proliferation assay. As detailed in Fig. 3, 48 h of exposure to parthenolide resulted in a dose-dependent inhibition of prostate cancer cell proliferation with an $IC_{50}$ of 4 μmol/liter (dose to inhibit proliferation to 50% of control) for both LNCaP and PC-3 cells.

**Immunohistochemistry.** Immunoreactive staining for the p65 subunit of NF-κB was cytoplasmic (Fig. 4). No immunoreactivity was seen in stromal cells. When the extent of staining in the normal, PIN, and adenocarcinoma specimens was quantified on the 0–3+ scale, there was a graded increase between the normal epithelial tissues, PIN, and cancer (Table 3). Specifically, none of the benign glands had 3+ and 66% exhibited 0 or 1+ staining. The amount of staining in the PIN lesions was intermediate with 74% of lesions having 1+ or 2+ and 25% had 3+. In contrast all of the cancer specimens were 2+ to 3+ (30 and 70%, respectively). The cancer specimens had no 0 or 1+. The difference in amount of staining was significantly greater in the PIN lesions compared with the benign glands ($P < 0.0001$) and was greater in the invasive neoplastic disease compared with the intraepithelial neoplasia ($P < 0.0001$).

Multiple pathological prognostic features and clinical parameters were correlated with the amount of staining (0–2+ *versus* 3+) in the cancer specimen. There was no association between T-stage, grade, prostate-specific antigen relapse, or extraprostatic extension. However, there was a trend toward an association between extent of tumor involvement in the prostatectomy and 3+ staining ($P = 0.056$).

## DISCUSSION

This data demonstrates the presence of constitutive NF-κB DNA binding in a variety of prostate cancer cells *in vitro* and that this can be inhibited by parthenolide. Of note is that the amount of NF-κB DNA binding is increased in LNCaP cells that have been in culture longer and the ratio of the p65:p50 heterodimer to p50:p50 homodimer is increased in the hormone-independent cell lines compared with the hormone-dependent cells. The p65:p50 heterodimer is more biologically active than other dimers and is associated with the antiapoptotic properties of NF-κB (18). This suggests that increased NF-κB activation may be associated with hormone independence. Also, the observation that cells that have been in culture longer develop an increase in NF-κB DNA binding may partially explain the observation by Igawa *et al.* (19) who have shown the LNCaP cell line becomes androgen independent with greater cell passages. Other investigators have found constitutive NF-κB DNA binding in prostate cancer cells *in vitro* and that NF-κB can be inhibited by a variety of agents, including selenium (20), ibu-

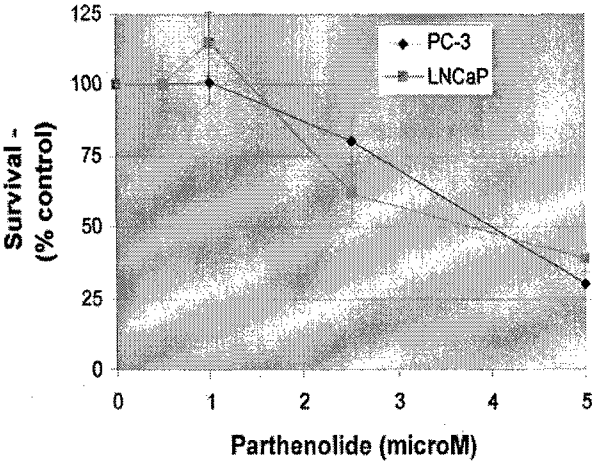


*Fig. 3* Proliferation assay with colorimetric proliferation assay demonstrating dose-dependent inhibition of prostate cancer cell proliferation with an NF-κB inhibitor, parthenolide.

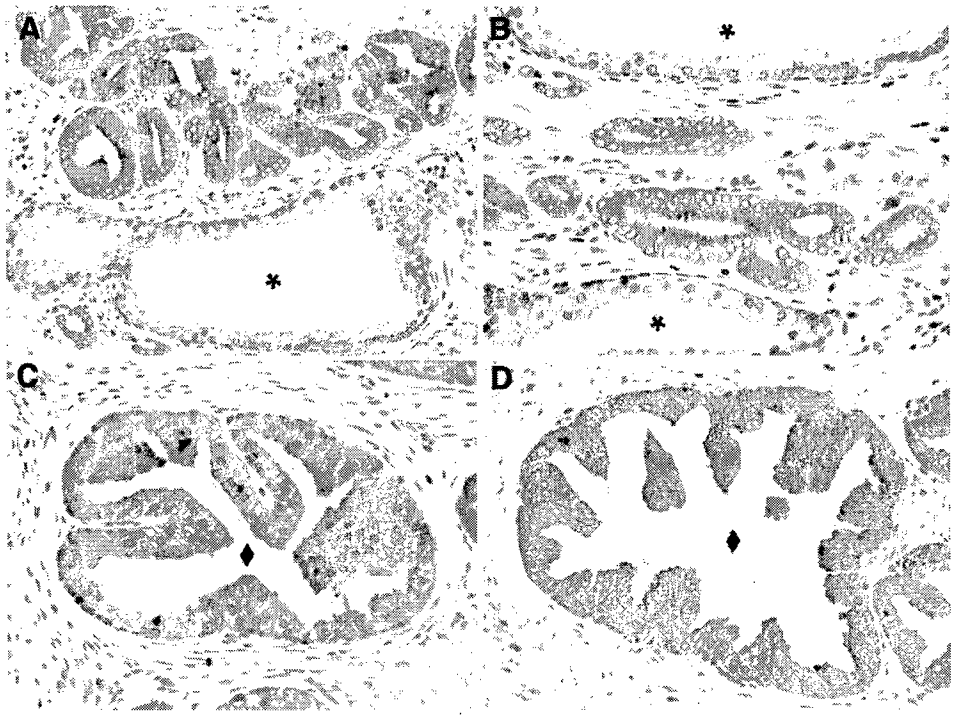


*Fig. 4* Photomicrograph of immunohistochemical staining of p65 (Santa Cruz Biotechnology) showing minimal immunoreactivity (intensity score of 1+) in benign prostate epithelium (*A* and *B*). In contrast, there is staining in the PIN: intensity score of 3+ (*C* and *D*). * indicates lumen of normal gland; ♦ indicates lumen of gland with PIN.

profen (21), ibdehydroxymethylepoxyquinomicin (22), dexamethasone (23), and genistein (24).

The relevance of NF-κB DNA binding in prostate cancer cells was confirmed by screening for the presence of and changes in genes under the control of NF-κB. We clearly have shown that many NF-κB-related genes that promote the cancer process are expressed in CWR22Rv1 cells and are decreased by the NF-κB inhibitor, parthenolide. The inhibition of NF-κB DNA binding was associated with an inhibition of cancer cell proliferation.

The p65 subunit is the more relevant component of NF-κB, and this article characterizes its location and frequency in human prostatectomy specimens by immunohistochemical staining. The differential staining (frequency and amount) and graded increase between the normal, PIN, and cancerous areas supports the contention that NF-κB is involved in carcinogenesis and, in particular, the genesis of prostate cancer. The presence of a high amount of staining in all of the prostate cancer specimens *in vivo* supports the *in vitro* electromobility gel shift assay data, which shows that increased NF-κB is a universal finding in prostate cancer and that it is involved in the development and propagation of prostate cancer (8, 11, 12, 25). The lack of nuclear staining is due either to the very short half-life of transcription factors in the nucleus or the fact NF-κB is increased in amount and is yet to be activated. Although this immunohistochemistry staining does not document the presence of activated NF-κB, it at least demonstrates that prostate cancer cells are primed to the deleterious effects of NF-κB activation by cytokines found in the prostate cancer microenvironment such as IL-$1_\alpha$ (26, 27). Our attempts to employ other antibodies that recognize an epitope that overlaps the nuclear localization signal of the p65 subunit, and hence identify released/activated NF-κB, were unsuccessful because of our inability to minimize the background staining (data not shown).

*Table 3* Staining intensity grade

| | Staining intensity grade ($N$ = 97) | | | |
|---|---|---|---|---|
| Intensity | 0 | 1 | 2 | 3 |
| Normal | 9 (9) | 57 (59) | 31 (32) | 0 (0) |
| PIN* | 1 (1) | 10 (10) | 62 (64) | 24 (25) |
| Cancer* | 0 (0) | 0 (0) | 29 (30) | 68 (70) |

NOTE. All data expressed as n (%)

* Indicates statistically different distribution of staining intensity compared with that of normal cells ($P < 0.0001$ using Wilcoxon paired signed rank test).

The lack of association between pathological and clinical prognostic features is probably due to the universal staining at either 2+ or 3+ intensity in the cancer cells. The presence of NF-κB in normal glands at a lower frequency and amount is because it is a ubiquitous transcription factor with a baseline level of activity to promote growth and survival of all cells. In contrast, the universal presence and higher amount in the cancer specimens suggests that this transcription process is involved in the malignant transformation. The observation of the sudden increase in NF-κB expression from the benign epithelium to the PIN lesions suggests that activation of NF-κB is an early event in prostate cancer carcinogenesis. Findings supporting this have been made in breast cancer. Specifically, carcinogen treatment of female Sprague Dawley rats *in vivo* and in human mammary epithelial cells in culture resulted in NF-κB activation just before malignant transformation of the breast tissue (28).

This article provides strong support for the hypothesis that NF-κB is increased and relevant at an early stage in prostate cancer because it is found in both PIN and cancerous lesions. This works provides support for the development of NF-κB inhibitors as either preventative agents (prevent the transition of normal cells to PIN or prevent the progression from PIN to cancer) or as a therapy for advanced prostate cancer.

## REFERENCES


1. Baeuerle PA, Henkel T. Function and activation of NF-kappaB in the immune system. Annu Rev Immunol 1994;12:141–79.

2. Garcia-Pineres AJ, Castro V, Mora G, et al. Cysteine 38 in p65/NF-kappaB plays a crucial role in DNA binding inhibition by sesquiterpene lactones. J Biol Chem 2001;276:39713–20.

3. Jones PL, Ping D, Boss JM. Tumor necrosis factor alpha and interleukin-1beta regulate the murine manganese superoxide dismutase gene through a complex intronic enhancer involving C/EBP-beta and NF-kappaB. Mol Cell Biol 1997;17:6970–81.

4. Zong WX, Edelstein LC, Chen C, Bash J, Gelinas C. The prosurvival Bcl-2 homolog Bfl-1/A1 is a direct transcriptional target of NF-kappaB that blocks TNFalpha-induced apoptosis. Genes Dev 1999;13:382–387.

5. Lee HH, Dadgostar H, Cheng Q, Shu J, Cheng G. NF-kappaB-mediated up-regulation of Bcl-x and Bfl-1/A1 is required for CD40 survival signaling in B lymphocytes. Proc Natl Acad Sci USA 1999; 96:9136–41.

6. Wang CY, Mayo MW, Baldwin, AS Jr. TNF- and cancer therapy-induced apoptosis: potentiation by inhibition of NF-kappaB. Science (Wash. DC) 1996;274:784–7.

7. Nakshatri H, Bhat-Nakshatri P, Martin DA, Goulet RJ Jr, Sledge GW Jr. Constitutive activation of NF-kappaB during progression of breast cancer to hormone-independent growth. Mol Cell Biol 1997;17: 3629–39.

8. Catz SD, Johnson JL. Transcriptional regulation of bcl-2 by nuclear factor kappa B and its significance in prostate cancer. Oncogene 2001; 20:7342–51.

9. Huang S, DeGuzman A, Bucana CD, Fidler IJ. Nuclear factor-kappaB activity correlates with growth, angiogenesis, and metastasis of human melanoma cells in nude mice. Clin Cancer Res 2000;6:2573–81.

10. Huang S, Robinson JB, Deguzman A, Bucana CD, Fidler IJ. Blockade of nuclear factor-kappaB signaling inhibits angiogenesis and tumorigenicity of human ovarian cancer cells by suppressing expression of vascular endothelial growth factor and interleukin 8. Cancer Res 2000; 60:5334–9.

11. Muenchen HJ, Lin DL, Walsh MA, Keller ET, Pienta KJ. Tumor necrosis factor-alpha-induced apoptosis in prostate cancer cells through inhibition of nuclear factor-kappaB by an IkappaBalpha "super-repressor." Clin Cancer Res 2000;6:1969–77.

12. Gupta S, Afaq F, Mukhtar H. Involvement of nuclear factor-kappa B, Bax and Bcl-2 in induction of cell cycle arrest and apoptosis by apigenin in human prostate carcinoma cells. Oncogene 2002;21: 3727–38.

13. Logothetis CJ, Yang H, Daliani D, et al. Dose-dependent inhibition of 20S proteasome results in serum IL-6 and PSA decline in patients with androgen independent prostate cancer treated with proteasome inhibitor PS 341. Proc Am Soc Clin Oncol 2001;20:186.

14. Adams J. Development of the proteasome inhibitor PS-341. Oncologist 2002;7:9–16.

15. Sramkoski RM, Pretlow TG II, Giaconia JM, et al. A new human prostate carcinoma cell line, 22Rv1. In Vitro Cell Dev Biol Anim 1999;35:403–9.

16. Pahl HL. Activators and target genes of Rel/NF-kappaB transcription factors. Oncogene 1999;18:6853–66.

17. Hanahan D, Weinberg RA. The hallmarks of cancer. Cell 2000; 100:57–70.

18. Chen X, Kandasamy K, Srivastava RK. Differential roles of RelA (p65) and c-Rel subunits of nuclear factor-kappaB in tumor necrosis factor-related apoptosis-inducing ligand signaling. Cancer Res 2003;63: 1059–66.

19. Igawa T, Lin FF, Lee MS, Karan D, Batra SK, Lin MF. Establishment and characterization of androgen-independent human prostate cancer LNCaP cell model. Prostate 2002;50:222–35.

20. Gasparian AV, Yao YJ, Lu J, et al. Selenium compounds inhibit I kappa B kinase (IKK) and nuclear factor-kappa B (NF-kappaB) in prostate cancer cells. Mol Cancer Ther 2002;1:1079–87.

21. Palayoor ST, Youmell MY, Calderwood SK, Coleman CN, Price BD. Constitutive activation of IkappaB kinase alpha and NF-kappaB in prostate cancer cells is inhibited by ibuprofen. Oncogene 1999;18: 7389–94.

22. Kikuchi E, Horiguchi Y, Nakashima J, et al. Suppression of hormone-refractory prostate cancer by a novel nuclear factor-kappaB inhibitor in nude mice. Cancer Res 2003;63:107–10.

23. Nishimura K, Nonomura N, Satoh E, et al. Potential mechanism for the effects of dexamethasone on growth of androgen-independent prostate cancer. J Natl Cancer Inst (Bethesda) 2001;93:1739–46.

24. Li Y, Sarkar FH. Inhibition of nuclear factor kappaB activation in PC3 cells by genistein is mediated via Akt signaling pathway. Clin Cancer Res 2002;8:2369–77.

25. Catz SD, Babior BM, Johnson JL. JFC1 is transcriptionally activated by nuclear factor-kappaB and up-regulated by tumour necrosis factor alpha in prostate carcinoma cells. Biochem J 2002;367:791–9.

26. Lee HL, Pienta KJ, Kim WJ, Cooper CR. The effect of bone-associated growth factors and cytokines on the growth of prostate cancer cells derived from soft tissue *versus* bone metastases *in vitro*. Int J Oncol 2003;22:921–6.

27. Ferrer FA, Miller LJ, Andrawis RI, et al. Angiogenesis and prostate cancer: *in vivo* and *in vitro* expression of angiogenesis factors by prostate cancer cells. Urology 1998;51:161–7.

28. Kim DW, Sovak MA, Zanieski G, et al. Activation of NF-kappaB/Rel occurs early during neoplastic transformation of mammary cells. Carcinogenesis (Lond.) 2000;21:871–9.